Journal of Applied Mechanics and Technical Physics, Vol. 47, No. 1, pp. 27–35, 2006

NUMERICAL SIMULATION OF PLASMA DYNAMICS IN A NONUNIFORM MAGNETIC FIELD

V. T. Astrelin,[1] A. V. Burdakov,[1] V. M. Kovenya,[2] and T. V. Kozlinskaya[3]

UDC 517.958:537.84

An efficient algorithm is proposed enabling numerical simulations of plasma dynamics in a nonuniform magnetic field. The present numerical data are in good agreement with experimental data obtained in a GOL-3 *setup and with previous simulations. The experimentally observed effect of fast transfer of energy to ions is confirmed.*

Key words: *numerical simulation, finite-difference scheme, plasma physics, magnetic field.*

Introduction. In GOL-3 experiments on plasma heating and confinement in a multiple-mirror trap, fast heating of plasma is ensured by a relativistic electron beam with an energy up to 1 MeV (current up to 30 kA, duration up to 8 μsec, and energy up to 120–150 kJ) [1]. A deuterium-plasma column of density $n \approx 10^{15}$ cm^{-3}, length of 12.3 m, and diameter of 4–5 cm is formed in a corrugated magnetic field consisting of 55 cells, each 22 cm long, with a magnetic ratio $B_{\max}/B_{\min} = 5.2/3.2$ T. The plasma column is confined by edge magnetic mirrors with a magnetic field of $B'_{\max} \approx 9$ T. Collective heating of the plasma by the beam proceeds under conditions of developed Langmuir turbulence and lengthwise electron heat conduction being suppressed by turbulent electric fields; in the corrugated field, such a situation gives rise to periodic longitudinal modulation of the electron temperature and pressure. The pressure gradient initiates formation and acceleration of plasma flows toward the centers of magnetic cells. Experiments showed that collisions between the flows result in neutron outbursts of thermonuclear nature, followed by fast thermalization of the directional energy of plasma motion accompanied by neutron emission [1]. Measurements confirmed a fast growth of ion energy (up to 1–2 keV for the period of beam action), which could not be explained by the Coulomb electron–ion collisions. To investigate the above-mentioned mechanism of fast transfer of energy to ions, the dynamics of a two-component plasma was numerically simulated in [2] with the use of traditional computational algorithms [3] in the hydrodynamic approximation, because the ion temperature in the plasma generated by a direct discharge in deuterium is low at the initial stage of heating and the free path of ions is much shorter than the length of one cell in the multiple-mirror trap. As a numerical analysis showed and an experiment confirmed [1], the dynamics of the plasma under such conditions is accompanied by generation of high-amplitude nonlinear waves, which requires more efficient algorithms to be developed to model the process of interest.

To numerically solve strongly nonlinear problems, algorithms with enhanced stability, capable of predicting solutions over long time intervals, are required (see [4]). Such algorithms can be developed on the basis of predictor–corrector schemes, where the required stability is ensured at the predictor stage and conservatism is re-established at the corrector stage, thus providing for satisfaction of differential conservation laws. A predictor–corrector scheme was proposed in [5, 6] for the numerical solution of gas-dynamic equations. The technique of splitting in terms of physical processes was used at the predictor stage in this scheme, which is used as the basic one in the present study.

[1]Budker Institute of Nuclear Physics, Siberian Division, Russian Academy of Sciences, Novosibirsk 630090. [2]Institute of Computational Technologies, Siberian Division, Russian Academy of Sciences, Novosibirsk 630090; kovenya@ict.nsc.ru. [3]Novosibirsk State University, Novosibirsk 630090; ktv-sun@gorodok.net. Translated from Prikladnaya Mekhanika i Tekhnicheskaya Fizika, Vol. 47, No. 1, pp. 35–45, January–February, 2006. Original article submitted March 28, 2005.

To ensure the second order of approximation over all variables, the starting equations were approximated at the corrector stage by symmetrical operators and a smoothing operator of the second-order smallness was introduced to retain monotonicity, as this was done in [7]. Test computations proved the scheme to be quite accurate and efficient.

Plasma heating with parameters close to the conditions of GOL-3 experiments with different configurations of the magnetic field was modeled in the present study with the use of the scheme described above. The numerical data obtained were compared with experimental results and data predicted by previous algorithms [1, 8].

Physicomathematical Model. The plasma dynamics is governed by the equations of continuity and motion (in the magnetized-plasma approximation) and by the energy equations for ions and electrons, which can be written in the following form for one-dimensional motion (see [2, 9, 10]):

$$\begin{gathered}
\frac{\partial n}{\partial t} + B\,\frac{\partial}{\partial z}\Big(\frac{nV}{B}\Big) = 0,\\
\frac{\partial V}{\partial t} + BV\,\frac{\partial}{\partial z}\Big(\frac{V}{B}\Big) + \frac{V^2}{B}\,\frac{\partial B}{\partial z} + \frac{1}{Mn}\,\frac{\partial}{\partial z}\,(nkT) = 0,\\
\frac{3}{2}\,\frac{\partial nT_{\mathrm{e}}}{\partial t} + B\,\frac{\partial}{\partial z}\Big(\frac{3}{2}\,\frac{nT_{\mathrm{e}}V}{B}\Big) + nT_{\mathrm{e}}B\,\frac{\partial}{\partial z}\Big(\frac{3}{2}\,\frac{V}{B}\Big) = \frac{\partial}{\partial z}\Big(\varkappa_{\mathrm{e}}\,\frac{\partial T_{\mathrm{e}}}{\partial z}\Big) + Q_{\mathrm{e}},\\
\frac{3}{2}\,\frac{\partial nT_{\mathrm{i}}}{\partial t} + B\,\frac{\partial}{\partial z}\Big(\frac{3}{2}\,\frac{nT_{\mathrm{i}}V}{B}\Big) + nT_{\mathrm{i}}B\,\frac{\partial}{\partial z}\Big(\frac{3}{2}\,\frac{V}{B}\Big) = \frac{\partial}{\partial z}\Big(\varkappa_{\mathrm{i}}\,\frac{\partial T_{\mathrm{i}}}{\partial z}\Big) + Q_{\mathrm{i}}.
\end{gathered} \tag{1}$$

System (1) is closed by the equations of state $p_{\mathrm{i}} = nkT_{\mathrm{i}}$ and $p_{\mathrm{e}} = nkT_{\mathrm{e}}$. The following notation is used: t is the time, z is the longitudinal coordinate along the line of magnetic force, n and V are the plasma density and velocity, M and m are the ion and electron masses, $M = 2M_{\mathrm{p}}$ (M_{p} is the proton mass), B is the magnetic induction, T_{e} and T_{i} are the electron and ion temperatures in the plasma, $T = T_{\mathrm{e}} + T_{\mathrm{i}}$, $p = p_{\mathrm{i}} + p_{\mathrm{e}}$ is the total pressure in the plasma, $\varkappa_{\mathrm{e}} = F_{\mathrm{e}}(Z_{\mathrm{eff}})nkT_{\mathrm{e}}\tau_{\mathrm{e}}/(\zeta m)$ and $\varkappa_{\mathrm{i}} = F_{\mathrm{i}}(Z_{\mathrm{eff}})nkT_{\mathrm{i}}\tau_{\mathrm{i}}/M$ are the longitudinal thermal conductivities with the collisional times τ_{e} and τ_{i} defined by the formulas [10]

$$\tau_{\mathrm{e}} = \frac{3\sqrt{m}\,(kT_{\mathrm{e}})^{3/2}}{4\sqrt{2\pi}\,\lambda e^4 n}, \qquad \tau_{\mathrm{i}} = \frac{3\sqrt{M}\,(kT_{\mathrm{i}})^{3/2}}{4\sqrt{\pi}\,\lambda e^4 n},$$

Z_{eff} is the effective ion charge due to impurities ($Z_{\mathrm{eff}} \approx 1$), the parameters $F_{\mathrm{e}} \approx 3.9$ and $F_{\mathrm{i}} \approx 4.4$ allow for variation of transport cross sections in the plasma with multicharged ions, k is the Boltzmann constant, λ is the Coulomb logarithm (in the case of interest, $\lambda \approx 13$), ζ is the heat-conduction suppression coefficient defined by the level of turbulence in the plasma: $\zeta = 1 + (\zeta_{\max} - 1)(P(t)/P_{\max})^2 R(n)$, $\zeta_{\max} \approx 10^2$–$10^3$ (experimentally found values), $P(t)$ is the beam power, $P_{\max}$ is the maximum beam power, $R(n) = f(n_b/n)$ is the experimentally measured loss in the beam energy, dependent on the ratio n_b/n and vanishing at beam-plasma instability increments lower than the electron–electron collisional frequency:

$$R(n) = \max\{0, 1 - \ln\,(n_{\mathrm{eff}}(z)/n^*)/\ln\,(n_{\mathrm{cr}}/n^*)\}.$$

Here $n_{\mathrm{eff}}(z) = \max\,(0.8, n(z)B_0/B(z))$, $n_{\mathrm{cr}} \approx (2\text{–}3)\cdot 10^{15}$ cm^{-3} is the critical plasma density above which no beam-induced turbulent heating of the plasma occurs, and $n^* \approx 0.8\cdot 10^{15}$ cm^{-3} is the plasma density below which the beam-energy losses in the heated plasma become almost independent of its density.

If the mean path of particles is commensurable with, or greater than, the pressure-nonuniformity length, one can use an approximate algorithm restricting the thermal conductivity by a restraint factor $\xi_\alpha(\varkappa_\alpha)$:

$$\varkappa_\alpha^{\mathrm{eff}} = \varkappa_\alpha \xi_\alpha(\varkappa_\alpha) = \varkappa_{\alpha,\max}(1 - \exp\,(-\varkappa_\alpha/\varkappa_{\alpha,\max})).$$

Here $\varkappa_{\alpha,\max} = q_{\alpha,\max}/|dT_\alpha/dz|$, $q_{\alpha,\max} = 3/(2\sqrt{\pi}\,)(nT_\alpha V_{T,\alpha})$ is the maximum possible heat flux due to particles, and $V_{T,\alpha} = (2kT_\alpha/m_\alpha)^{1/2}$ is the thermal velocity of particles; $\alpha = \mathrm{e}, \mathrm{i}$ is the type of particles.

The sources $Q_{\mathrm{e,i}}$ describe the variation of energy in the plasma components

$$Q_{\mathrm{e}} = Q_0 + n\nu_\varepsilon^{\mathrm{e/i}}(T_{\mathrm{i}} - T_{\mathrm{e}}), \qquad Q_{\mathrm{i}} = n\nu_\varepsilon^{\mathrm{i/e}}(T_{\mathrm{e}} - T_{\mathrm{i}}), \tag{2}$$

where $\nu_\varepsilon^{\mathrm{e/i}} = \nu_\varepsilon^{\mathrm{i/e}} = 4.75\cdot 10^{-9} Z_{\mathrm{eff}}^2 n\lambda M_{\mathrm{p}}/(MT_{\mathrm{e}}^{3/2})$ [cm^3/sec] is the electron–ion collisional frequency. The term Q_0 in Eq. (2) describes plasma heating by electrons of the beam (with an efficiency η_1) and by epithermal electrons

of the plasma, generated by the beam during its turbulent interaction with the plasma, whose typical energy ("temperature") is $T_h \approx 10$ keV (with an efficiency η_2):

$$Q_0 = \frac{P(t)B(z)}{S_0 B_0^* L}\,[\eta_1 R_{\text{eff}}(n,z) + \eta_2 \Phi(n,z,T_h)].$$

Here $R_{\text{eff}}(n,z) = AR(n)(1 + (K_n - 1)l_0/(z + l_0))$, K_n and l_0 are parameters that characterize the longitudinal heating nonuniformity resulting from beam spreading over velocities in the plasma (in the experiment, $K_n \approx 2.9$ and $l_0 = 2$ m), B_0^* is the magnetic induction in the section S_0, L is the length of the system, and A is a normalization factor such that $\dfrac{1}{L}\displaystyle\int_0^L R_{\text{eff}}(n,z)\,dz = 1$.

The component Φ describes plasma heating due to relaxation of the fast "tail" of plasma electrons:

$$\Phi(n,z,T_h) = \frac{0.85nL}{2R_0(T_h)} \int\limits_{\varepsilon'_{\min}}^{\infty} \psi(\xi,\varepsilon')\,d\varepsilon'.$$

Here $\varepsilon' = \varepsilon/T_h$ is the dimensionless energy of fast electrons, $\varepsilon'_{\min}$ is the energy at which the mean path of electrons $R_0(\varepsilon)$ [cm^{-2}] $= 2.5 \cdot 10^{18} \cdot \varepsilon^2$ [keV]$/\lambda$ equals $\langle nl\rangle = \displaystyle\int_0^z n(l)\,dl$, $\xi = \langle nl\rangle/R_0(\varepsilon)$, and $\psi(\xi,\varepsilon') = 3.39 \times (0.01 + \xi)^{0.25} \exp(-6\xi^{2.5} - \varepsilon')$ is the dimensionless function of energy absorption for epithermal electrons in the target. The coefficient 0.85 takes into account partial reflection of epithermal electrons from the edge magnetic mirrors.

For convenience of numerical integration, we bring Eq. (1) to dimensionless form by choosing the following quantities typical of the initial state of the plasma as the starting parameters: length $L_0 = 10^2$ cm, time $t_0 = 10^{-6}$ sec, velocity $V_0 = 10^8$ cm/sec, magnetic field $B_0 = 1$ T, density $n_0 = 10^{15}$ cm^{-3}, temperature $T_0 = 10^3$ eV, and beam power $P_0 = 10^9$ W. All quantities below are mostly presented as dimensionless quantities.

The functions to be found are chosen to be the plasma density and velocity, the ion pressure, and the total pressure. Then the system under consideration can be written in dimensionless form as

$$\begin{gathered}
\frac{\partial n}{\partial t} + V\frac{\partial n}{\partial z} + Bn\frac{\partial}{\partial z}\Big(\frac{V}{B}\Big) = 0,\\
\frac{\partial V}{\partial t} + V\frac{\partial V}{\partial z} + \frac{A_0}{n}\frac{\partial p}{\partial z} = 0,\\
\frac{\partial p_{\text{i}}}{\partial t} + V\frac{\partial p_{\text{i}}}{\partial z} + \gamma B p_{\text{i}}\frac{\partial}{\partial z}\Big(\frac{V}{B}\Big) = \frac{\partial}{\partial z}\Big(\tilde{\xi}_{\text{i}}\frac{\partial T_{\text{i}}}{\partial z}\Big) + \frac{A_1}{\gamma'}\,(p - 2p_{\text{i}}),\\
\frac{\partial p}{\partial t} + V\frac{\partial p}{\partial z} + \gamma B p\frac{\partial}{\partial z}\Big(\frac{V}{B}\Big) = \frac{\partial}{\partial z}\Big(\tilde{\xi}_{\text{e}}\frac{\partial T}{\partial z}\Big) + F_0,
\end{gathered} \tag{3}$$

where $\gamma = 5/3$, $\gamma' = \gamma - 1$, $\tilde{\xi}_{\text{i}} = K_{\text{i}}\xi_{\text{i}}T_{\text{i}}^{5/2}/\gamma'$, $\tilde{\xi}_{\text{e}} = K_{\text{e}}\xi_{\text{e}}T_{\text{e}}^{5/2}/(\gamma'\zeta)$ are the temperature-dependent thermal conductivities, $A_0 = (C_0^2/V_0^2)M_{\text{p}}/M$ and $A_1 = 1.3014 \cdot 10^{-3} Z_{\text{eff}}^2 M_{\text{p}}/(\tilde{T}_{\text{e}}^{3/2} M)$ are dimensionless parameters, $C_0 = \sqrt{\gamma p/(nM)}$ is the velocity of ion-sound waves in the plasma, and $F_0 = \tilde{Q}_0/\gamma' + \partial\,((\tilde{\xi}_{\text{i}} - \tilde{\xi}_{\text{e}})\,\partial T_{\text{i}}/\partial z)/\partial z$.

We rewrite system (3) in the vector form

$$\frac{\partial f}{\partial t} + \Omega f = F, \tag{4}$$

where

$$f = \begin{pmatrix} n \\ V \\ p_{\text{i}} \\ p \end{pmatrix}; \qquad F = \begin{pmatrix} 0 \\ 0 \\ 0 \\ F_0 \end{pmatrix};$$

$$\Omega = \begin{pmatrix} V\dfrac{\partial}{\partial z} & Bn\dfrac{\partial}{\partial z}\dfrac{1}{B} & 0 & 0 \\ 0 & V\dfrac{\partial}{\partial z} & 0 & \dfrac{A_0}{n}\dfrac{\partial}{\partial z} \\ 0 & \gamma Bp_{\rm i}\dfrac{\partial}{\partial z}\dfrac{1}{B} & V\dfrac{\partial}{\partial z} - \dfrac{\partial}{\partial z}\tilde{\xi}_{\rm i}\dfrac{\partial}{\partial z}\dfrac{1}{n} + 2A_1 & -A_1 \\ 0 & \gamma Bp\dfrac{\partial}{\partial z}\dfrac{1}{B} & 0 & V\dfrac{\partial}{\partial z} - \dfrac{\partial}{\partial z}\tilde{\xi}_{\rm e}\dfrac{\partial}{\partial z}\dfrac{1}{n} \end{pmatrix}.$$

We seek for the solution of system (4) in the domain $\Pi = \{z_0 \leqslant z \leqslant L,\, t > 0\}$. The boundary conditions at the edges of the system, controlled by free outflow of the plasma through the edge magnetic mirrors, can be approximately represented as follows (see [2]):

$$\frac{\partial nT_{\rm e,i}}{\partial z}\Big|_{z=0,L} = 0, \qquad \frac{\partial V}{\partial z}\Big|_{z=0,L} = 0, \qquad T_{\rm e,i}\Big|_{z=0,L} = \max\left(T_{0\rm e,i}, 0.05T_{\rm e,i}^{\max}\right). \tag{5}$$

Initially, the system is filled by a cold plasma:

$$T_{0\rm e,i} = 1 \text{ eV}, \qquad n_0 = 10^{15} \text{ cm}^{-3}, \qquad V_0 = 0.$$

Difference System. The domain Π is covered by a computational grid with constant steps h and τ. The operator Ω is approximated by the difference operator Ω_h:

$$\Omega_h = \begin{pmatrix} V\Lambda & Bn\Lambda\dfrac{1}{B} & 0 & 0 \\ 0 & V\Lambda & 0 & \dfrac{A_0}{n}\bar{\Lambda} \\ 0 & \gamma Bp_{\rm i}\Lambda\dfrac{1}{B} & V\Lambda - \Lambda\tilde{\xi}_{\rm i}\Lambda\dfrac{1}{n} + 2A_1 & -A_1 \\ 0 & \gamma Bp\Lambda\dfrac{1}{B} & 0 & V\Lambda - \Lambda\tilde{\xi}_{\rm e}\Lambda\dfrac{1}{n} \end{pmatrix}.$$

Here

$$\Lambda = \begin{cases} \Lambda_- & \text{if} \quad V \geqslant 0, \\ \Lambda_+ & \text{if} \quad V < 0; \end{cases} \qquad \bar{\Lambda} = \begin{cases} \Lambda_+ & \text{if} \quad V \geqslant 0, \\ \Lambda_- & \text{if} \quad V < 0; \end{cases}$$

$\Lambda_\pm f_j = \pm(f_{j\pm1} - f_j)/h$ is the approximation of the first derivative, with due regard for the sign of V^l, with the order $O(h)$, and $\Lambda a\Lambda$ is the approximation of the second derivatives by a three-point symmetric operator. As in [5, 6], the operator Ω_h is represented as the sum $\Omega_h = \Omega_{1h} + \Omega_{2h}$, where

$$\Omega_{1h} = \begin{pmatrix} V\Lambda & Bn\Lambda\dfrac{1}{B} & 0 & 0 \\ 0 & V\Lambda & 0 & 0 \\ 0 & 0 & 0 & 0 \\ 0 & 0 & 0 & 0 \end{pmatrix}; \quad \Omega_{2h} = \begin{pmatrix} 0 & 0 & 0 & 0 \\ 0 & 0 & 0 & \dfrac{A_0}{n}\bar{\Lambda} \\ 0 & a_{\rm i}\Lambda\dfrac{1}{B} & V\Lambda - \Lambda\tilde{\xi}_{\rm i}\Lambda\dfrac{1}{n} + 2A_1 & -A_1 \\ 0 & a\Lambda\dfrac{1}{B} & 0 & V\Lambda - \Lambda\tilde{\xi}_{\rm e}\Lambda\dfrac{1}{n} \end{pmatrix}.$$

With the notation used, the difference scheme

$$\begin{gathered} \frac{f^{l+1/4} - f^l}{\tau\alpha} + \Omega_{1h}f^{l+1/4} = 0, \qquad \frac{f^{l+1/2} - f^{l+1/4}}{\tau\alpha} + \Omega_{2h}f^{l+1/2} = 0, \\ \frac{f^{l+1} - f^l}{\tau} + \tilde{\Omega}_h f^{l+1/2} = F^{l+1/2} \end{gathered} \tag{6}$$

approximates the starting equations (4) with the order $O(\tau^m + \tau h + h^k)$, where $m = 2$ for $\alpha = 0.5 + O(\tau)$ and $m = 1$ for $\alpha \neq 0.5$; k is the order of approximation of the operator Ω_h at the corrector stage. To improve the

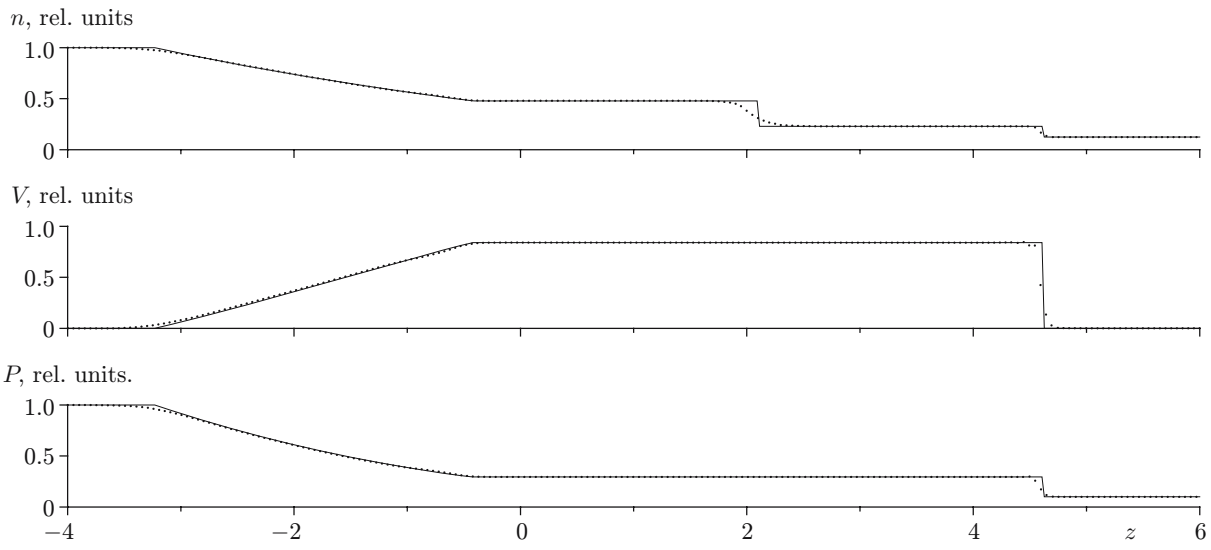

Fig. 1

computation accuracy, we approximate the operator Ω at the corrector stage by a symmetric operator with the second order. Then, the difference scheme (6) approximates the starting equations (4) with the order $O(\tau^2 + h^2)$ at $\alpha = 0.5 + O(\tau)$. By virtue of the symmetric approximation of the vector of the operator $\tilde{\Omega}_h$, the scheme turns out to be nonmonotonic; to eliminate oscillations, a smoothing second-order operator is introduced at the corrector stage, as was done in [7]:

$$\Lambda af = \frac{(af)_{j+1} - (af)_{j-1}}{2h} - \frac{h}{2}\,\frac{b_{j+1/2}\Lambda_+ f_j - b_{j-1/2}\Lambda_- f_j}{h}. \tag{7}$$

Here $b_{j\pm1/2} = (b_{j\pm1} + b_j)/2$ and $b_j = \varepsilon^2|a_j|$; $\varepsilon = 0$ if $d = 0$ and $\varepsilon = |f_{j+1} - 2f_j + f_{j-1}|/d$ if $d = |f_{j+1} - f_j| + |f_j - f_{j-1}|$.

In the linear approximation with $F = 0$, the difference scheme (6) is unconditionally stable for $\alpha \geqslant 0.5$. As it follows from the form of the matrix operators Ω_{jh}, this scheme is implemented through scalar three-point sweeps at fractional steps and in an explicit manner at the corrector steps.

Note that the solution stability and the possibility of simulating the formation and collision of strongly nonlinear waves in previous algorithms were provided by introducing an artificial viscosity and by smoothing local disturbances arising in the difference scheme used [2], which could affect the quality of the data obtained. The algorithm described above involves no artificial viscosity.

Schemes (4)–(7) were tested by solving two problems: the Riemann problem and a steady flow through a variable-section channel. In the first problem, the initial and boundary conditions were set as follows:

$$\begin{aligned} &n(z,0) = 1, \quad V(z,0) = 0, \quad p(z,0) = 1 && \text{for} \quad -4 \leqslant z \leqslant 0; \\ &n(z,0) = 0.125, \quad V(z,0) = 0, \quad p(z,0) = 0.1 && \text{for} \quad 0 < z \leqslant 6; \end{aligned}$$

$$n(-4,t) = 1, \quad V(-4,t) = 0, \quad p(-4,t) = 1, \quad n(6,t) = 0.125, \quad V(6,t) = 0, \quad p(6,t) = 0.1.$$

Note that system (6) with $F \equiv 0$ and $p_\mathrm{i} = p$, $p_\mathrm{e} = 0$, and $\tilde{\zeta}_\mathrm{i} = \tilde{\zeta}_\mathrm{e} = 0$ is a gas-dynamic system in a quasi-one-dimensional approximation, with B^{-1} understood as the cross-sectional area of the channel. Obviously, for $B = \mathrm{const}$, Eqs. (4) form a system of one-dimensional time-dependent gas-dynamic equations.

Figure 1 shows the data computed by the second-order scheme (6) with the smoothing operator (7) at the time $t = 2.5$ on a computational grid containing 200 nodes over z with $\alpha = 0.505$. The solid and dotted curves show the exact solution and the numerical solution, respectively. The shock wave is seen to be smeared over 2–3 nodes, and the contact discontinuity is spread over 6 nodes. The scheme adequately predicts the velocities of the shock and rarefaction waves. A similar result was also obtained with the first-order scheme; in the latter case, however, the contact discontinuity is spread over 10–12 nodes. The computations were performed for the Courant

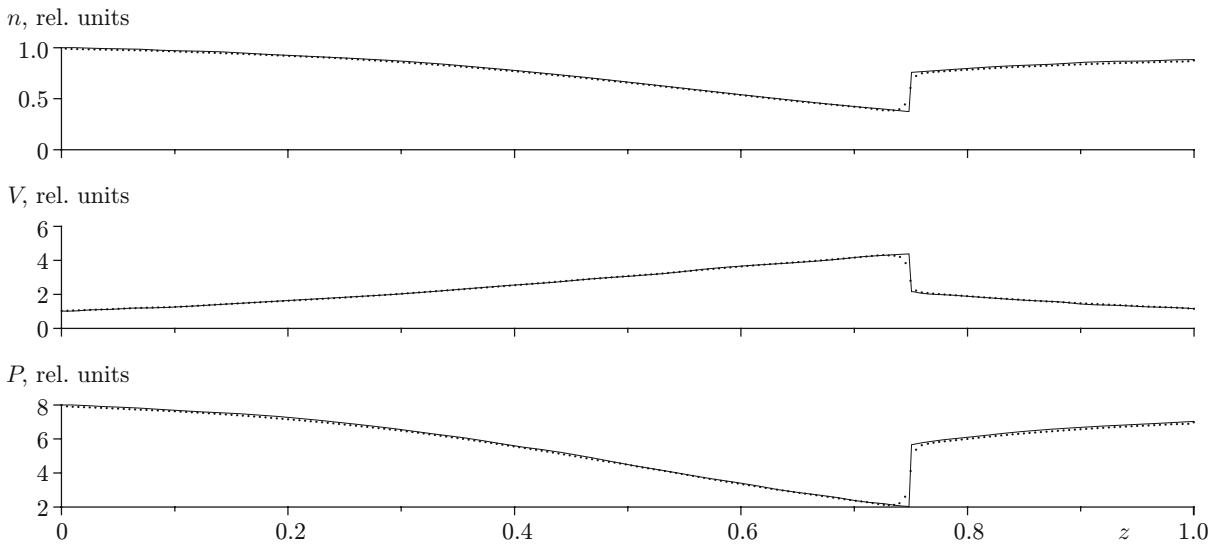

Fig. 2

number $k = \max(\tau|V \pm c|/h) = 1$. All data below were also obtained by the second-order scheme with solution monotonization.

In the problem of a quasi-one-dimensional steady flow through a variable-section channel described by the formula $B(x) = 0.5 + 0.5(1-2x)^2$ $(0 \leqslant x \leqslant 1)$, the solution was obtained numerically by a time-dependent method. Initially $(t = 0)$, the values of the function at the channel entrance and exit were set to satisfy the exact solution

$$\begin{pmatrix} n \\ V \\ p \end{pmatrix}_{x=0} = \begin{pmatrix} 1 \\ 1.0237 \\ 8 \end{pmatrix}, \qquad \begin{pmatrix} n \\ V \\ p \end{pmatrix}_{x=1} = \begin{pmatrix} 0.8835 \\ 1.1586 \\ 7.0315 \end{pmatrix}.$$

The solution involves a discontinuity of gas-dynamic quantities. Figure 2 shows the exact and numerical solutions (solid and dotted curves, respectively) after stabilization of the solution by scheme (6) on a computational grid consisting of 200 nodes. As the computed data show, the proposed scheme allows obtaining fairly accurate solutions of stationary and nonstationary problems with flow discontinuities and singularities.

Simulation of Plasma Heating and Motion. To test the algorithms and their capability in modeling the plasma-heating mechanism within the framework of the proposed physical model [2], we simulated plasma dynamics under conditions of a special GOL-3 experiment with a single magnetic cell [11, 12]. Undisturbed values of the sought quantities were initially $(t = 0)$ set in a channel of length $L = 12.32$ m: $n = 1$, $V = 0$, and $T_\mathrm{i} = T_\mathrm{e} = 0.001$. The external magnetic field was specified as $B = 2 + \cos(2(z - 1.5\pi))$ for $1.5\pi \leqslant z \leqslant 2.5\pi$ and as $B = 3$ for $0 \leqslant z \leqslant 1.5\pi$ and $2.5\pi \leqslant z \leqslant 12.3$. The system was assumed to be open, to admit free outflow of the plasma at the channel edges, and to satisfy the boundary conditions (5). To find the numerical solution of Eqs. (4), we used the predictor–corrector scheme (6) with the order $O(\tau^2 + h^2)$. The computational grid contained 400 modes over the coordinate z. As was noted above, the difference scheme (6) is unconditionally stable in the absence of external forces. Yet, with external sources F, which were explicitly computed at the corrector stage, the difference scheme can lose the property of unconditional stability. In the latter case, the time parameter τ can be found from the scheme stability in terms of the right side. Owing to the contribution of beam-induced heating to the source term F, the latter becomes the determining term in the energy equation, prevailing over convective and other terms. In this situation, the electron temperature sharply increases (approximately by a factor of 1000). The computations were performed for the Courant number $k \approx 0.01$–0.1 admitted by stability of the scheme. Figure 3 shows the distributions of velocity, density, electron temperature, and total temperature at the times $t = 1$, 2, 3, and 4 μsec (curves 1, 2, 3, and 4, respectively) for the prescribed distribution of the magnetic field.

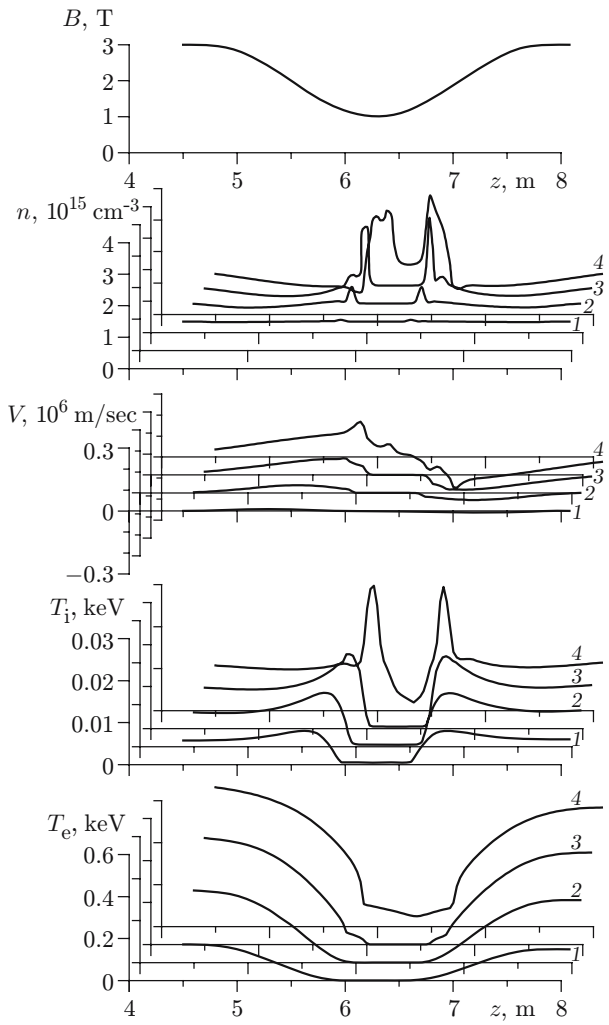

Fig. 3

In accordance with the hypothetical mechanism of ion acceleration and with the GOL-3 experimental data (see [11]), the plasma is heated nonuniformly by the electron beam because of the magnetic-field nonuniformity: the temperature increases rather appreciably at the edges of the mirror system and to a smaller extent at the center of the well. The nonuniformity of pressure results in acceleration of the plasma toward the center of the cell. At $t > 4$ μsec, the two flows collide and, as estimates show, penetrate each other.

Within the framework of the single-velocity model under consideration, the computations by the above-described algorithm yielded the following results. In solving the problem, the electron-beam-induced plasma heating causes a substantial (by a factor of 1000) increase in electron temperature of the plasma; the maximum increase is observed outside the magnetic well (see Fig. 3). The ion temperature increases approximately tenfold and reaches its maximum values at the edges of the magnetic well. Owing to plasma acceleration toward the center of the magnetic well, the density increases in the well (by a factor of 2.8 compared to the initial data) and decreases outside the well. The total pressure is completely determined by the electron pressure: it increased to a greater extent at the well edges of the well than in the center. The maximum kinetic energy of accelerated ions reaches approximately 0.3–0.5 of the electron temperature, which is consistent with experimental observations. The numerical solution is both qualitatively and quantitatively close to those obtained in the experiment and in previous simulations (see [2, 11]) up to the time $t = 4$ μsec. For times $t > 4$ μsec, however, the computations predict that two plasma flows collide at the center of the well, causing a drastic increase in temperature and pressure. The single-velocity model becomes invalid for such times, and multiflow models should be used to compute such flows.

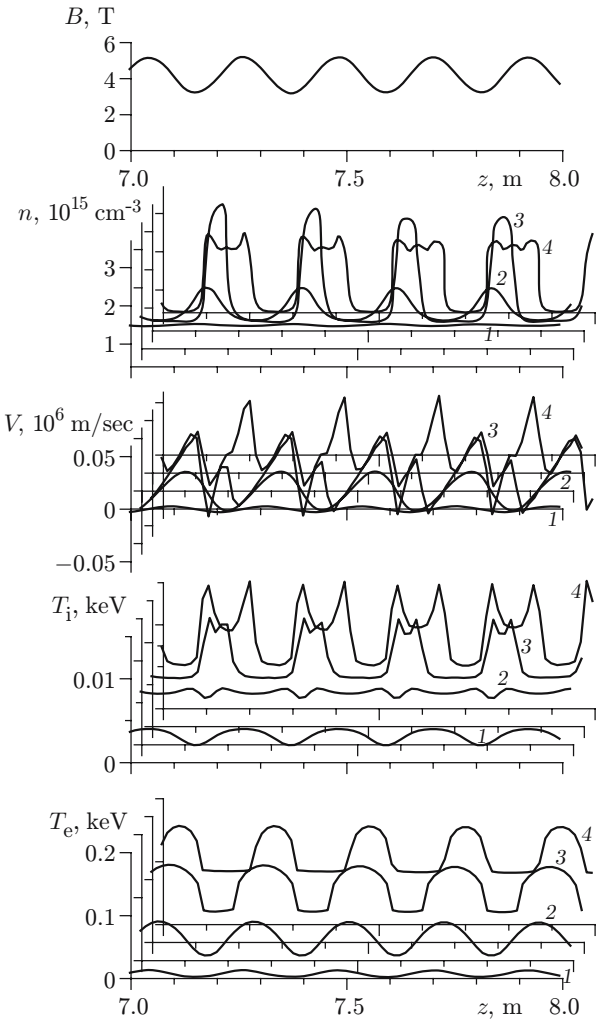

Fig. 4

Result Computed for a Multiple Mirror Magnetic-Field Configuration. To test the algorithms and examine the mechanism of collective acceleration of ions, we also solved the problem with a periodic magnetic field close to that in the GOL-3 multiple mirror trap. Two goals were pursued in the simulation. The first goal was to expand the stable solution domain, which was significantly restricted by the capability of previously used numerical algorithm in earlier computations. The second goal was to examine the influence of the degree of nonuniformity of electron-beam-induced heating on the longitudinal uniformity of ion acceleration (in the model, this influence can be specified using experimentally measured data).

In the simulation, the external magnetic field in each field cell was set as $B = 4.2 + \cos(2\pi z/0.22)$ [T] in the interval $0.11 \leqslant z \leqslant 12.21$ and $B = 6.1 + 2.9\cos(2\pi z/0.22)$ [T] outside this interval. This definition corresponded to a multiple mirror trap with a total length of 12.32 m, which was restricted by two edge mirrors with a magnetic field of 9 T. The system contained a total of 56 such magnetic cells spaced by 22 cm. The computational grid consisted of 1000 nodes over the coordinate z. Each cell contained 18 nodes. Undisturbed values of the sought quantities were initially set in a channel of length $L = 12.32$ m: $n = 1.5 \cdot 10^{15}$ cm^{-3}, $V = 0$, and $T_\mathrm{e} = T_\mathrm{i} = 1$ eV. Figure 4 shows the distributions of velocity, density, electron temperature, and total temperature $T = T_\mathrm{e} + T_\mathrm{i}$ at the times $t = 0.5$, 1, 1.5, and 1.8 μsec (curves 1, 2, 3, and 4, respectively) in the corrugated magnetic field.

As the density of the magnetized beam varies in proportion to the magnetic field, the ratio n_b/n, which determines the efficiency of heating of plasma electrons also periodically varies along the system at $t = 0$. At the

ends of each cell, where the magnetic field is high, effective heating of the plasma by the beam is observed. At the center of each cell, the beam-to-plasma density ratio becomes lower than the value required for development of beam-plasma turbulence, and the local heating of the plasma is much lower. As a result, the developing electron-pressure nonuniformity accelerates the plasma toward the midplane, giving rise to accelerated ion counter-flows from regions with a high magnetic field in each cell toward its midplane. The collective acceleration of ions observed enhances their kinetic energy to values comparable with the thermal energy of electrons to values comparable with the thermal energy of electrons in a time shorter than the beam duration. The distribution of plasma parameters obtained in the present computations complies with simulation data previously obtained by other algorithms up to computation times of 1.8 μsec. The proposed hydrodynamic model for the multiple mirror trap is valid only till the moments at which plasma counter-flows collide. Like in the case of the single-cell magnetic-field configuration, one has to use multiflow or kinetic models for times $t > 1.8$ μsec.

Conclusions. A physicomathematical model is proposed to predict strongly nonlinear processes in the dynamics of high-temperature plasma under electron-beam heating confined in an open trap with a nonuniform magnetic field. Highly efficient algorithms based on the splitting technique are developed and tested. The accuracy of the algorithms is estimated by solving problems with discontinuous solutions. Actual GOL-3 experiments are numerically simulated. Good agreement between the present simulation data and result obtained in experiments and in previous simulation studies is reached. The latter proves the capability of the chosen physicomathematical model to predict the mechanism of plasma heating up to the moment the plasma flows collide with each other. Validity of the chosen model and adequacy of numerical data obtained by different numerical algorithms are demonstrated. The experimentally observed effect of fast transfer of energy to ions is confirmed. The necessity of application of kinetic models for predicting plasma dynamics over long times is shown.

This work was partially supported by the Russian Foundation for Basic Research (Grant No. 05-01-00146a) and by the Siberian Division of the Russian Academy of Sciences (Integration Project Nos. 148 and 162).

REFERENCES

1. A. V. Burdakov, A. V. Arzhannikov, V. T. Astrelin, et al., "Fast heating of ions in GOL-3 multiple mirror trap," in: *Proc. of the 31th Conf. on Controlled Fusion and Plasma Physics* (London, June 28–July 2, 2004) [CD-ROM], Vol. 27A, European Physical Society (2004), p. P4-156.
2. V. T. Astrelin, A. V. Burdakov, V. S. Koidan, and V. V. Postupaev, "Dynamics of plasma heated by electron beam in corrugated magnetic field," in: *Proc. of the 30th Conf. on Controlled Fusion and Plasma Physics* (St. Petersburg, Russia, July 7–11, 2003) [CD-ROM], Vol. 27A, European Physical Society (2003), p. P-2.192.
3. A. A. Samarskii and Yu. P. Popov, *Difference Schemes in Gas Dynamics* [in Russian], Nauka, Moscow (1975).
4. V. M. Kovenya, *Difference Methods for Solving Multidimensional Problems* [in Russian], Izd. Novosib. Univ., Novosibirsk (2004).
5. V. M. Kovenya and A. S. Lebedev, "Modified splitting technique for constructing efficient difference schemes," *Zh. Vychisl. Mat. Mat. Fiz.*, **34**, No. 6, 886–897 (1994).
6. V. M. Kovenya and T. V. Kozlinskaya, "Calculation algorithm for electron-beam-induced plasma heating," *Vychisl. Tekhnol.*, **9**, No. 6, 59–67 (2004).
7. V. M. Kovenya and A. S. Lebedev, "Numerical study of the near-wake separated flow," Preprint No. 14-87, Inst. of Theoretical and Applied Mechanics, USSR Acad. of Sci., Novosibirsk (1987).
8. A. V. Arzhannikov, V. T. Astrelin, A. V. Burdakov, et al. "Dynamics of ions of a beam-heated plasma in a cell of multimirror open trap," *Trans. Fus. Technol.*, **43**, No. 1T, 172–176 (2003).
9. L. A. Artsimovich and R. Z. Sagdeev, *Plasma Physics for Physicists* [in Russian], Atomizdat, Moscow (1979).
10. S. I. Braginskii, "Transport phenomena in plasma," in: *Problems in Plasma Theory* [in Russian], Vol. 1, Gosatomizdat, Moscow (1963), pp. 183–272.
11. A. V. Arzhannikov, V. T. Astrelin, A. V. Burdakov, et al., "Direct observation of anomalously low longitudinal electron heat conduction during collective relaxation of a high-current relativistic electron beam in the plasma," *Pis'ma Zh. Éksp. Teor. Fiz.*, **77**, No. 7, 426–429 (2003).
12. R. Yu. Akentev, A. V. Arzhannikov, V. T. Astrelin, et al., "Experimental results on multiple mirror trap GOL-3," in: *Proc. of the 29th Conf. on Controlled Fusion and Plasma Physics* (Montreux, July 1–5, 2002) [CD-ROM], Vol. 26B, European Physical Society (2002), p. P-5.057.